Journal of Solid State Chemistry 182 (2009) 586–591

Contents lists available at ScienceDirect

Journal of Solid State Chemistry

journal homepage: www.elsevier.com/locate/jssc

Nuclear magnetic resonance study of hydrogen mobility in $LaY_2Ni_9H_x$ and $CeY_2Ni_9H_x$

A.V. Soloninin [a], A.L. Buzlukov [a], A.V. Skripov [a,*], M. Latroche [b], V. Paul-Boncour [b]

[a] Institute of Metal Physics, Urals Branch of the Academy of Sciences, S. Kovalevskoi 18, Ekaterinburg 620041, Russia
[b] Chimie Métallurgique des Terres Rares, Institut de Chimie et des Matériaux de Paris Est, CNRS, 2-8 rue H. Dunant, 94320 Thiais, France

ARTICLE INFO

Article history:
Received 9 September 2008
Received in revised form
28 November 2008
Accepted 13 December 2008
Available online 24 December 2008

Keywords:
Metal hydrides
Diffusion
Nuclear magnetic resonance

ABSTRACT

In order to investigate the mobility of hydrogen in the ternary compounds LaY_2Ni_9 and CeY_2Ni_9, we have measured the proton nuclear magnetic resonance (NMR) spectra and the proton spin–lattice relaxation rates R_1 for $LaY_2Ni_9H_x$ ($x = 0.78$ and 10.3) and $CeY_2Ni_9H_x$ ($x = 0.79$ and 7.2). The measurements have been performed at the resonance frequencies of 14, 23.8 and 90 MHz over the temperature range of 11–404 K. For $LaY_2Ni_9H_x$, the behavior of R_1 is consistent with the presence of a considerable contribution due to motionally modulated dipole–dipole interaction between nuclear spins. This contribution can be satisfactorily described in terms of the Bloembergen–Purcell–Pound model with a Gaussian distribution of activation energies for hydrogen diffusion; the value of the average activation energy resulting from such a description for $LaY_2Ni_9H_{10.3}$ is approximately 0.36 eV. For $CeY_2Ni_9H_x$ compounds, the measured proton spin–lattice relaxation rates are dominated by the contribution due to the interaction between proton spins and paramagnetic centers over the entire temperature range studied. Only qualitative information on H mobility in these compounds has been obtained from the narrowing of NMR spectra. Possible paths of H diffusion in $LaY_2Ni_9H_x$ and $CeY_2Ni_9H_x$ are discussed in terms of the distances between the interstitial sites occupied by hydrogen.

1. Introduction

The new family of ternary intermetallic compounds RM_2Ni_9 (R = rare earth or Ca, M = Mg, Ca, Ti or Y) [1–5] crystallize in the ordered modification of $PuNi_3$-type rhombohedral structure (space group $R\bar{3}m$). This structure can be described as a stacking of $CaCu_5$-type (Haucke phase) and $MgZn_2$-type (Laves phase) units along the c axis. The compounds LaY_2Ni_9 and CeY_2Ni_9 belonging to this family can absorb large amounts of hydrogen (up to 13 H atoms and 9 H atoms per formula unit of LaY_2Ni_9 and CeY_2Ni_9, respectively) [4]. Both compounds have a rather narrow concentration range of a solid-solution phase (up to ~0.8 H atoms per formula unit). Neutron diffraction study of the concentrated hydride phases of $LaY_2Ni_9D_{12.8}$ and $CeY_2Ni_9D_{7.7}$ [6] has shown that although the structures of both phases can be described in terms of the $R\bar{3}m$ space group, there is a significant difference between them. In $LaY_2Ni_9D_{12.8}$ hydrogen atoms occupy interstitial sites in both $CaCu_5$-type and $MgZn_2$-type units, and the lattice expansion due to hydrogenation is nearly isotropic ($\delta c/c = 9.7\%$, $\delta a/a = 7.2\%$) [6]. In $CeY_2Ni_9D_{7.7}$ hydrogen atoms occupy interstitial sites in $MgZn_2$-type units only, while $CaCu_5$-type layers remain empty. Such an unusual distribution of hydrogen is accompanied by the strongly anisotropic lattice distortion due to hydrogenation: the lattice parameter c in $CeY_2Ni_9D_{7.7}$ is 27.6% longer than in CeY_2Ni_9, while the lattice parameter a in the hydride is 2.0% *shorter* than in the hydrogen-free compound [6]. Similar structural features were earlier reported for $CeNi_3D_{2.7}$ [7] with the orthorhombic host-metal structure (space group *Pmcn*). Study of the magnetic properties of LaY_2Ni_9 and CeY_2Ni_9 compounds and their hydrides [8] has shown that both LaY_2Ni_9 and CeY_2Ni_9 are ferromagnets with the Curie temperatures $T_C = 15$ and 92 K, respectively. The hydride phase $LaY_2Ni_9H_{12}$ becomes a Pauli paramagnet, whereas $CeY_2Ni_9H_8$ remains ferromagnetic with $T_C = 77$ K and an additional magnetic contribution of trivalent Ce atoms belonging to the $MgZn_2$-type units occupied by hydrogen atoms [8,9].

The rate of H diffusion in materials may affect the kinetics of hydrogen absorption/desorption, being an important factor of the applicability of these materials for hydrogen storage. Hydrogen mobility in $PuNi_3$-type compounds has not been studied so far. Since nuclear magnetic resonance (NMR) is known as an effective microscopic method for investigation of H jump motion [10], it seems natural to apply NMR to study the rate of hydrogen diffusion in this new family of intermetallic hydrides. The aim of the present work is to study the mobility of hydrogen in $LaY_2Ni_9H_x$ and $CeY_2Ni_9H_x$ using proton NMR. We have measured the proton NMR spectra and spin–lattice relaxation rates for both

* Corresponding author. Fax: +7 343 374 5244.
E-mail address: skripov@imp.uran.ru (A.V. Skripov).

0022-4596/$ - see front matter © 2009 Elsevier Inc. All rights reserved.
doi:10.1016/j.jssc.2008.12.006

the solid-solution and hydride phases of $LaY_2Ni_9H_x$ and $CeY_2Ni_9H_x$ over the temperature range of 11–404 K.

2. Experimental details

The preparation of RY_2Ni_9 alloys (R = La, Ce) was analogous to that described in [4]. The alloys were prepared by induction melting of pure components (3N purity) under vacuum in a water-cooled copper crucible. The samples were melted five times to ensure good homogeneity. They were then annealed at 750 °C for 3 weeks and quenched to room temperature. The composition and the homogeneity of the alloys were checked by electron probe microanalysis and X-ray diffraction. Hydrogenation was performed from the gas phase by Sievert's method based on pressure variation measurements in calibrated and temperature controlled volumes; this method allows accurate determination of the H content. Four samples with the compositions $LaY_2Ni_9H_{0.78}$, $LaY_2Ni_9H_{10.3}$, $CeY_2Ni_9H_{0.79}$ and $CeY_2Ni_9H_{7.2}$ were chosen for NMR measurements. According to X-ray diffraction analysis, all these hydrogenated samples retained $PuNi_3$-type structure of the host lattice. For NMR experiments, the powdered samples were sealed in glass tubes under argon.

NMR measurements were performed on a modernized Bruker SXP pulse spectrometer at the frequencies $\omega/2\pi = 14$, 23.8 and 90 MHz. A probehead with the sample was placed into an Oxford Instruments CF1200 continuous-flow cryostat using helium or nitrogen as cooling agents. The sample temperature, monitored by a chromel-(Au–Fe) thermocouple, was stable to ± 0.1 K. The proton NMR spectra were recorded by Fourier transforming the spin echo signals. The proton spin–lattice relaxation rates R_1 were measured using the saturation–recovery method. In all cases the recovery of the nuclear magnetization could be satisfactorily described by a single-exponential function.

3. Results and discussion

The measured proton spin–lattice relaxation rate R_1 in metal–hydrogen systems is usually determined by the sum of contributions resulting from the interactions of proton spins with conduction electrons (R_{1e}) and paramagnetic centers (R_{1p}) and from the internuclear dipole–dipole interactions modulated by H motion (R_{1d}) [10]. The frequency-independent electronic (Korringa) contribution R_{1e} is typically proportional to the temperature, $R_{1e} = C_eT$. For Pauli paramagnets, the electronic contribution dominates at low temperatures, while the motional contribution R_{1d} becomes more important in the temperature range where the H jump rate τ_d^{-1} is between 10^7 and 10^{11} s^{-1}. The temperature dependence of R_{1d} shows a characteristic peak at the temperature at which $\omega\tau_d \approx 1$. In the limit of slow H diffusion ($\omega\tau_d \gg 1$), R_{1d} is proportional to $\omega^{-2}\tau_d^{-1}$, and in the limit of fast H diffusion ($\omega\tau_d \ll 1$), R_{1d} is proportional to τ_d being frequency-independent. The behavior of the paramagnetic contribution R_{1p} is more complex; it depends on a number of parameters [11] including the spin–lattice relaxation time of paramagnetic ions τ_i.

3.1. $LaY_2Ni_9H_x$ compounds

The temperature dependences of the proton spin–lattice relaxation rates measured at $\omega/2\pi = 14$, 23.8 and 90 MHz for $LaY_2Ni_9H_{10.3}$ are shown in Fig. 1. At $T < 200$ K, the measured relaxation rates are nearly frequency-independent, and their temperature dependence can be reasonably described by the linear function C_eT+B with $C_e = 2.3 \times 10^{-2}$ s^{-1} K^{-1} and $B = 0.77$ s^{-1}. This low-temperature behavior of R_1 is typical of metallic systems with small concentrations of paramagnetic centers. The coefficient C_e is proportional to the square of the density of electron states at the Fermi level; C_e values of the order of 10^{-2} s^{-1} K^{-1} have been found for many metal–hydrogen systems [10]. The term B can be identified as the low-temperature limit of the paramagnetic contribution R_{1p}. The frequency-dependent increase in R_1 at $T > 250$ K (Fig. 1) should be attributed to H jump motion that becomes fast enough to contribute strongly to the measured relaxation rate. However, the characteristic $R_1(T)$ peak has not been reached in our measurements up to 364 K. Because of a possible H desorption, we have not performed any measurements above 364 K for the hydrides and above 404 K for the solid solutions.

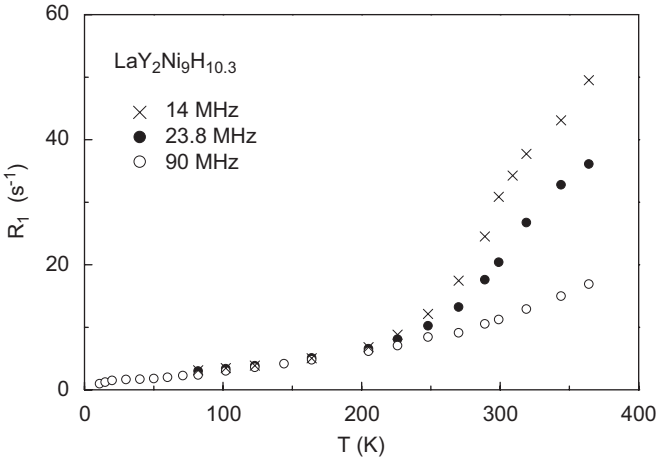

Fig. 1. The temperature dependences of the proton spin–lattice relaxation rates measured at 14, 23.8 and 90 MHz for $LaY_2Ni_9H_{10.3}$.

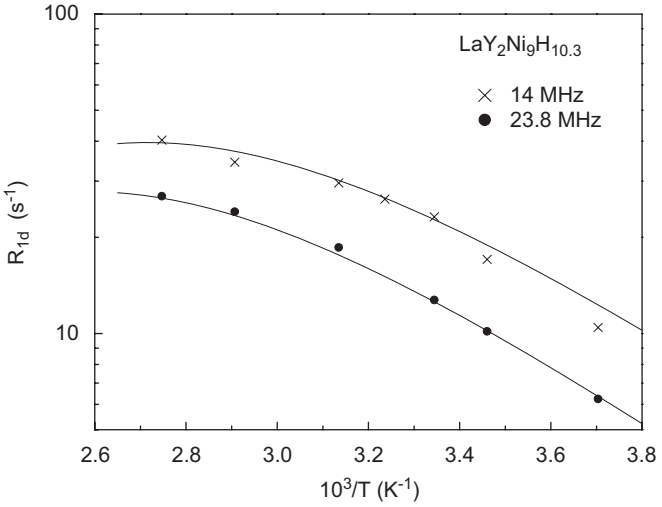

Fig. 2. The dipolar contributions to the proton spin–lattice relaxation rates at 14 and 23.8 MHz as functions of the inverse temperature for $LaY_2Ni_9H_{10.3}$. The solid curves show the simultaneous fits of the BPP model with a Gaussian distribution of activation energies to the data.

In order to estimate the parameters of H jump motion, we have to determine the temperature dependence of the motional contribution R_{1d}, i.e., to subtract R_{1e}+R_{1p} from the experimental results. This procedure is usually based on extrapolation of the low-temperature (C_eT+B) data. The behavior of R_{1d} at $\omega/2\pi = 14$ and 23.8 MHz resulting from such a subtraction is shown in Fig. 2 as a function of the inverse temperature. It should be noted that the frequency dependence of R_{1d} at the low-temperature slope of

the relaxation rate peak is considerably weaker than the expected ω^{-2} dependence. This feature often indicates the presence of a certain distribution of τ_d^{-1} values. Therefore, for parametrization of the data we have used the Bloembergen–Purcell–Pound (BPP) model with a Gaussian distribution of the activation energies E_a [12,13]. In the framework of this model, the temperature dependence of R_{1d} is determined by the pre-exponential factor τ_{d0}^{-1} of the Arrhenius law for the H jump rate, the average activation energy $\overline{E}_a$ and the distribution width (dispersion) ΔE_a. We look for a set of parameters giving the best fit to $R_{1d}(T)$ at two resonance frequencies *simultaneously*. The results of such simultaneous fits are shown by full curves in Fig. 2. The corresponding fit parameters are $\tau_{d0}^{-1} = 9.1 \times 10^{12}\,\mathrm{s}^{-1}$, $\overline{E}_a = 0.362\,\mathrm{eV}$ and $\Delta E_a = 0.055\,\mathrm{eV}$. For comparison, typical values of E_a for the long-range H diffusion in $MgZn_2$-type Laves-phase hydrides are in the range of 0.13–0.19 eV [14–16]. Thus, although the structure of LaY_2Ni_9 includes $MgZn_2$-type units, the mobility of hydrogen in the hydride of LaY_2Ni_9 is much lower than in typical Laves-phase hydrides. Since a part of H atoms in $LaY_2Ni_9H_x$ occupy interstitial sites in $CaCu_5$-type units, it is also interesting to compare the H mobility in $LaY_2Ni_9H_x$ with that in the hydride of $LaNi_5$. According to the proton NMR measurements [17,18], the spin–lattice relaxation rate in $LaNi_5H_6$ shows the characteristic peak near room temperature, and the activation energy for the long-range H diffusion in $LaNi_5H_6$ is about 0.29–0.31 eV. These results indicate that the mobility of hydrogen in LaY_2Ni_9 hydride is also somewhat lower than in $LaNi_5$ hydride.

In order to discuss possible paths of hydrogen jump motion in $LaY_2Ni_9H_x$, we have to consider the distances between the sites partially occupied by hydrogen atoms. According to the neutron diffraction data for $LaY_2Ni_9D_{12.8}$ [6], hydrogen atoms in this compound occupy eight types of interstitial sites: $6c_3$ (Ni_4), $18h_2$ ($LaYNi_2$), $18h_3$ (Y_2Ni_2), $18h_6$ (YNi_3), $36i_1$ (Y_2Ni_2), $6c_4$ (Ni_4), $18h_5$ ($LaNi_3$) and $36i_2$ ($LaNi_3$). The coordination of these sites shown in the brackets corresponds to the ideally ordered metallic sublattice with La atoms fully occupying $3a$ sites and Y atoms fully occupying $6c$ sites of the $PuNi_3$-type structure; in reality, there is a certain degree of La–Y mixing [4,6]. The sites $6c_3$, $18h_2$, $18h_3$, $18h_6$ and $36i_1$ belong to $MgZn_2$-type structural units, while the sites $6c_4$, $18h_5$ and $36i_2$ are in $CaCu_5$-type units. The structure of $LaY_2Ni_9D_{12.8}$ is schematically shown in Fig. 3 (left). Table 1 shows the distances (shorter than 1.8 Å) within the hydrogen sublattice, as derived from the neutron diffraction data for $LaY_2Ni_9D_{12.8}$ [6]. Since all the distances included in Table 1 are shorter than the 'blocking' radius of ~2.1 Å [19], each pair of sites separated by these distances can be populated by only one H atom at any given moment. For Laves-phase hydrides, it has been shown that the hydrogen jump rate between a certain pair of sites strongly increases with the decreasing distance between these sites [14]. Therefore, one may expect higher H jump rates for shorter intersite distances. As can be seen from Table 1, the network of interstitial sites partially occupied by hydrogen in $LaY_2Ni_9H_x$ has many short contacts between the nearest neighbors. In particular, the sites in $MgZn_2$-type and $CaCu_5$-type structural units are connected via short distances $6c_3$–$6c_4$, $18h_2$–$18h_5$ and $18h_3$–$18h_5$. The existence of a broad distribution of the nearest-neighbor intersite distances in Table 1 is consistent with our interpretation of the proton spin–lattice relaxation data in terms of the model implying a broad distribution of H jump rates. It should be noted that the sublattices of $36i_1$ and $36i_2$ sites consist of pairs of sites with the nearest-neighbor distances as small as 0.39 Å for $36i_1$ and 0.25 Å for $36i_2$. The jump rates of H motion with such small jump lengths (which are comparable to the hydrogen vibration amplitudes) are expected to be much higher than those found in our R_1 measurements. It is probable that, instead of forming such split states, H atoms are located at the centers of these pairs. This location is practically impossible to distinguish from the occupation of the $36i_1$ and $36i_2$ pairs on the basis of analysis of neutron diffraction patterns. Table 1 shows that, in terms of intersite distances, $LaY_2Ni_9H_x$ appears to be as favorable for fast H diffusion as $MgZn_2$-type Laves-phase hydrides (for comparison, see the intersite distances for some $MgZn_2$-type compounds in Table 1 of Ref. [16]). Our results suggest that some other factors may be

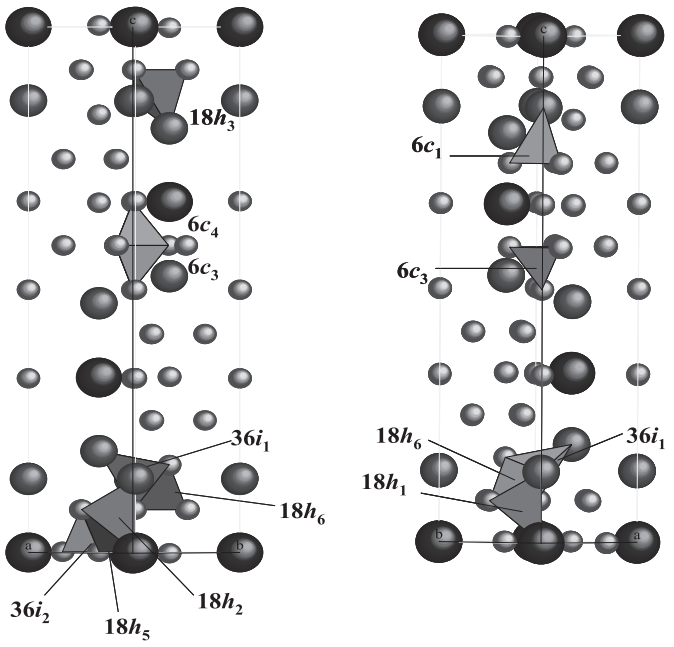

Fig. 3. The crystal structures of $LaY_2Ni_9D_{12.8}$ (left) and $CeY_2Ni_9D_{7.7}$ (right) with the vertically oriented c axis. Large black spheres: La and Ce atoms; middle gray spheres: Y atoms; small light gray spheres: Ni atoms. The crystallographic sites occupied by hydrogen atoms are shown as tetrahedra labeled according to their Wyckoff positions (space group $R\bar{3}m$).

Table 1
The distances (in Å) between the interstitial sites partially occupied by hydrogen atoms in $LaY_2Ni_9D_{12.8}$.

Sites	$6c_3$	$18h_2$	$18h_3$	$18h_6$	$36i_1$	$6c_4$	$18h_5$	$36i_2$
$6c_3$				0.99 (3)		1.34 (1)		
$18h_2$			1.02 (1)				0.72 (1)	
$18h_3$		1.02 (1)	1.62 (2)		1.48 (2), 1.68 (2)		1.41 (1)	
$18h_6$	0.99 (1)			1.62 (2)	1.43 (2), 1.63 (2)			
$36i_1$			1.48 (1), 1.68 (1)	1.43 (1), 1.63 (1)	0.39 (1)			
$6c_4$	1.34 (1)							1.79 (6)
$18h_5$		0.72 (1)	1.41 (1)					
$36i_2$						1.79 (1)		0.25 (1), 1.05 (1), 1.08 (1)

Only the distances shorter than 1.8 Å are shown. The number of the neighbors at the same distance is shown in parentheses. The table is read horizontally, e.g., the $6c_3$ site has three nearest-neighbor $18h_6$ sites at a distance of 0.99 Å.

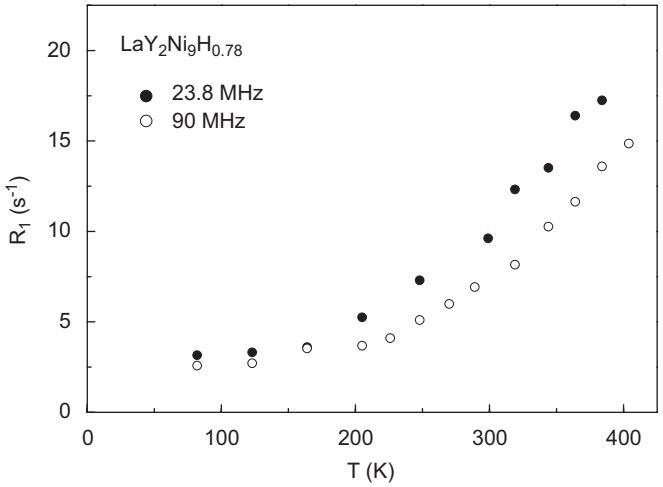

Fig. 4. The temperature dependences of the proton spin–lattice relaxation rates measured at 23.8 and 90 MHz for $LaY_2Ni_9H_{0.78}$.

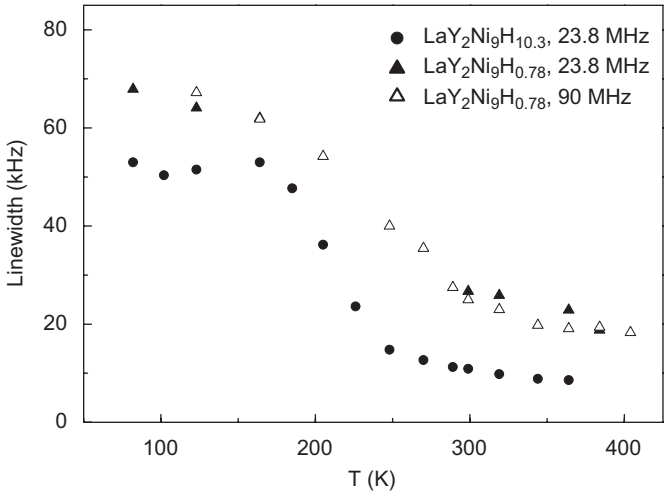

Fig. 5. The temperature dependences of the width (full width at half-maximum) of the proton NMR spectra measured at 23.8 MHz for $LaY_2Ni_9H_{10.3}$ and at 23.8 and 90 MHz for $LaY_2Ni_9H_{0.78}$.

responsible for higher activation barriers for H diffusion in LaY_2Ni_9, for example, strong distortions of some tetrahedra coordinating the interstitial sites and/or a certain degree of disorder (La–Y mixing) in the 3*a* and 6*c* metal sublattices.

The temperature dependences of the proton spin–lattice relaxation rates measured at 23.8 and 90 MHz for $LaY_2Ni_9H_{0.78}$ (solid-solution phase) are shown in Fig. 4. As in the case of $LaY_2Ni_9H_{10.3}$, the frequency-dependent increase in R_1 at $T>200$ K for $LaY_2Ni_9H_{0.78}$ can be attributed to the growth of the motional contribution R_{1d}. However, the observed frequency dependence of R_1 in the temperature range of 300–360 K for $LaY_2Ni_9H_{0.78}$ is considerably weaker than that for $LaY_2Ni_9H_{10.3}$, and it is difficult to separate different contributions to R_1 and estimate the parameters of H motion on the basis of the data presented in Fig. 4.

Additional information on H motion can, in principle, be obtained from the behavior of the width of ^{1}H NMR line. Fig. 5 shows the temperature dependences of the proton NMR linewidth (full width at half-maximum) for $LaY_2Ni_9H_{10.3}$ and $LaY_2Ni_9H_{0.78}$. For $LaY_2Ni_9H_{10.3}$ the linewidth is nearly constant at low temperatures ($T<160$ K); with increasing temperature it drops sharply near 200 K and reaches the new plateau at $T>320$ K. Such a behavior is typical of many metal–hydrogen systems. The line narrowing becomes pronounced above the temperature at which the H jump rate exceeds the 'rigid-lattice' (low-temperature) linewidth [20]. Therefore, the T range of sharp line narrowing can characterize the H jump rate on the frequency scale of tens of kHz. Since the spin–lattice relaxation is sensitive to higher H jump rates, the onset of a marked increase in R_{1d} should be observed at somewhat higher temperatures than the sharp line narrowing. This is consistent with the experimental data for $LaY_2Ni_9H_{10.3}$ (Figs. 1 and 5). For different compounds, the faster H jump motion should correspond to the lower T range of line narrowing. As can be seen from Fig. 5, for $LaY_2Ni_9H_{0.78}$ the significant line narrowing is observed in nearly the same T range as for $LaY_2Ni_9H_{10.3}$. However, for the solid-solution phase the transition range is broader and the linewidth at the high-temperature plateau is considerably larger than for the hydride phase. The proton linewidth at the high-temperature plateau in metal–hydrogen systems is usually determined by a distribution of demagnetizing fields over the sample volume [20,21], while the internuclear dipole–dipole interaction in this range is completely averaged out due to fast H diffusion. In this case one would expect a strong increase in the linewidth with the increasing external magnetic field (or the resonance frequency). While this is true for $LaY_2Ni_9H_{10.3}$ (not shown), for $LaY_2Ni_9H_{0.78}$ the observed proton linewidth at the high-temperature plateau is nearly the same at $\omega/2\pi = 23.8$ and 90 MHz (Fig. 5). This frequency independence indicates that the proton linewidth in the plateau range is determined by the dipole–dipole interaction, and a rather high plateau value of the linewidth suggests that the motion responsible for the line narrowing in $LaY_2Ni_9H_{0.78}$ is localized, since such a motion leads to only partial averaging of dipole–dipole interactions. It may be expected that the long-range H diffusion on the NMR frequency scale is excited in the solid-solution sample at still higher temperatures.

3.2. $CeY_2Ni_9H_x$ compounds

The temperature dependences of the proton spin–lattice relaxation rates measured at 14, 23.8 and 90 MHz for $CeY_2Ni_9H_{7.2}$ and at 23.8 and 90 MHz for $CeY_2Ni_9H_{0.79}$ are shown in Fig. 6. Comparison with the corresponding data for the La-based compounds (Figs. 1 and 4) indicates that the relaxation rates for $CeY_2Ni_9H_x$ are much higher than those for $LaY_2Ni_9H_x$ and exhibit qualitatively different temperature dependence. Indeed, in contrast to the case of $LaY_2Ni_9H_x$, the proton spin–lattice relaxation rates for both $CeY_2Ni_9H_x$ compounds decrease with the increasing temperature. These features suggest that the dominant contribution to the measured proton spin–lattice relaxation rate in $CeY_2Ni_9H_x$ is due to the interaction between nuclear spins and paramagnetic centers. This is consistent with the results of Ref. [8] showing that the magnetization of $CeY_2Ni_9H_x$ is considerably higher than that of $LaY_2Ni_9H_x$, especially below 150 K. Therefore, the parameters of H jump motion for the Ce-based compounds cannot be determined from the proton spin–lattice relaxation data. However, the temperature dependences of the proton NMR linewidths in $CeY_2Ni_9H_x$ (Fig. 7) still show the characteristic narrowing due to H motion. Comparison of the linewidth data for $CeY_2Ni_9H_{7.2}$ (Fig. 7) and for $LaY_2Ni_9H_{10.3}$ (Fig. 5) indicates that for the Ce-based hydride the characteristic 'step' is somewhat smeared out, and the onset of the line narrowing is shifted to higher temperature from that for the La-based hydride. Thus, we can conclude that in the temperature range of 200–300 K, the hydrogen mobility in $CeY_2Ni_9H_{7.2}$ is somewhat lower than that in $LaY_2Ni_9H_{10.3}$. As can be seen from Fig. 7, the significant line narrowing for $CeY_2Ni_9H_{0.78}$ is observed in nearly the same T range

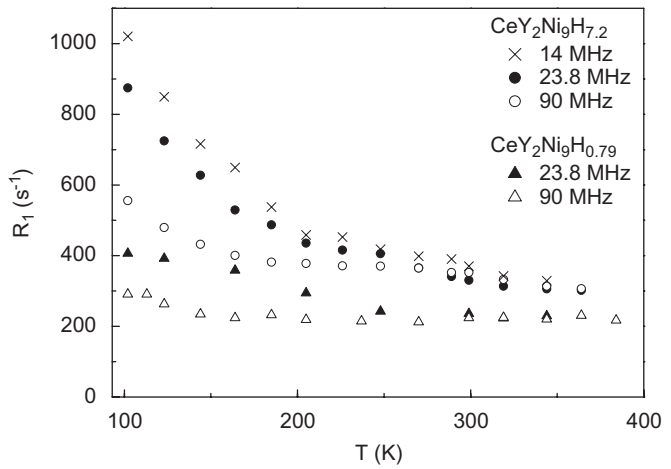

Fig. 6. The temperature dependences of the proton spin–lattice relaxation rates measured at 14, 23.8 and 90 MHz for $CeY_2Ni_9H_{7.2}$ and at 23.8 and 90 MHz for $CeY_2Ni_9H_{0.79}$.

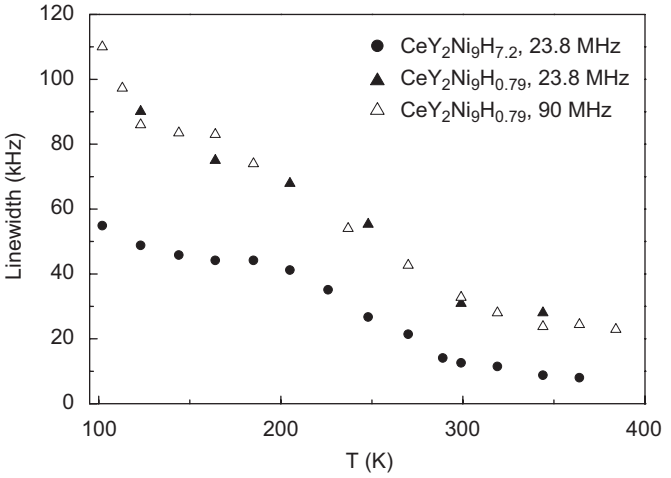

Fig. 7. The temperature dependences of the width (full width at half-maximum) of the proton NMR spectra measured at 23.8 MHz for $CeY_2Ni_9H_{7.2}$ and at 23.8 and 90 MHz for $CeY_2Ni_9H_{0.79}$.

as for $CeY_2Ni_9H_{7.2}$. However, for the solid-solution phase the transition range is somewhat broader, and the linewidth at the high-temperature plateau is larger than for the hydride phase. The same arguments, as in the case of $LaY_2Ni_9H_{0.79}$, suggest that the H motion responsible for the observed line narrowing in $CeY_2Ni_9H_{0.78}$ is localized.

According to the neutron diffraction data for $CeY_2Ni_9D_{7.7}$ [6], hydrogen atoms in this compound occupy five types of interstitial sites in $MgZn_2$-type structural units: $6c_1$ ($(Ce,Y)Ni_3$), $6c_3$ (Ni_4), $18h_1$ ($(Ce,Y)_2Ni_2$), $18h_6$ ($(Ce,Y)Ni_3$) and $36i_1$ ($(Ce,Y)_2Ni_2$). The coordination of these sites shown in the brackets reflects the fact that Ce and Y atoms in CeY_2Ni_9 are randomly distributed over the $3a$ and $6c$ metal sublattices [4,6]. The structure of $CeY_2Ni_9D_{7.7}$ is schematically shown in Fig. 3 (right). Table 2 shows the distances (shorter than 1.8 Å, except for $6c_1$–$36i_1$) within the hydrogen sublattice, as derived from the neutron diffraction data for $CeY_2Ni_9D_{7.7}$ [6]. The $6c_1$–$36i_1$ distance of 2.45 Å is included in Table 2, since this is the shortest distance between the $6c_1$ site and other sites partially occupied by hydrogen. While the $6c_1$ sites are somewhat separated from the other sites, the network of $6c_3$, $18h_1$, $18h_6$ and $36i_1$ has many short contacts between the nearest

Table 2
The distances (in Å) between the interstitial sites partially occupied by hydrogen atoms in $CeY_2Ni_9D_{7.7}$.

Sites	$6c_1$	$6c_3$	$18h_1$	$18h_6$	$36i_1$
$6c_1$					2.45 (6)
$6c_3$				0.52 (3)	
$18h_1$			1.68 (2)	1.53 (1)	
$18h_6$		0.52 (1)	1.53 (1)	0.69 (2)	
$36i_1$	2.45 (1)				0.33 (1), 1.18 (1), 1.45 (2), 1.72 (1)

Except for $6c_1$–$36i_1$, only the distances shorter than 1.8 Å are shown. The number of the neighbors at the same distance is shown in parentheses. The table is read horizontally, e.g., the $6c_1$ site has six nearest-neighbor $36i_1$ sites at a distance of 2.45 Å.

neighbors. Comparison of Tables 1 and 2 shows that the values of the nearest-neighbor distances between common types of sites ($6c_3$–$18h_6$, $18h_6$–$18h_6$ and $36i_1$–$36i_1$) for the hydrides of LaY_2Ni_9 and CeY_2Ni_9 differ significantly. For example, the $6c_3$–$18h_6$ distance is 0.99 Å for the La-based hydride and 0.52 Å for the Ce-based hydride. Such a difference originates from the difference in the hydrogen-induced lattice expansion, which is nearly isotropic for LaY_2Ni_9 and strongly anisotropic for CeY_2Ni_9. As in the case of $LaY_2Ni_9H_x$, the existence of pairs of $36i_1$ sites separated by 0.33 Å (Table 2) suggests that hydrogen atoms may be actually located in the centers of such pairs.

4. Conclusions

The results of our proton NMR measurements for $LaY_2Ni_9H_x$ ($x = 0.78$ and 10.3) and $CeY_2Ni_9H_x$ ($x = 0.79$ and 7.2) indicate that the hydrogen mobility in these compounds is considerably lower than in typical Laves-phase hydrides and somewhat lower than in $LaNi_5$ hydrides. For $LaY_2Ni_9H_{10.3}$ the experimental proton spin–lattice relaxation data can be satisfactorily described in terms of the BPP model with a Gaussian distribution of activation energies for H diffusion; the value of the average activation energy derived from such a description is approximately 0.36 eV. For $CeY_2Ni_9H_x$ compounds, the measured proton spin–lattice relaxation rates are dominated by the contribution due to the interaction between proton spins and paramagnetic centers over the entire temperature range studied. Therefore, qualitative information on H mobility in $CeY_2Ni_9H_x$ can only be obtained from the proton NMR line narrowing. The analysis of the distances between the sites partially occupied by hydrogen in $LaY_2Ni_9H_x$ and $CeY_2Ni_9H_x$ suggests that these compounds should be as favorable for fast H diffusion as $MgZn_2$-type Laves-phase hydrides. Thus, the higher barriers for H diffusion in $LaY_2Ni_9H_x$ and $CeY_2Ni_9H_x$ cannot be explained just in terms of intersite distances; other factors of electronic and/or structural origin have to be invoked.

Acknowledgments

This work was partially supported by the Russian Foundation for Basic Research (Grant no. 06-02-16246) and by the Priority Program 'Basic energy problems' of the Russian Academy of Sciences.

References

[1] K. Kadir, T. Sakai, I. Uehara, J. Alloys Compd. 257 (1997) 115.
[2] K. Kadir, T. Sakai, I. Uehara, J. Alloys Compd. 302 (2000) 112.
[3] J. Chen, H.T. Takeshita, H. Tanaka, N. Kuriyama, T. Sakai, I. Uehara, M. Haruta, J. Alloys Compd. 302 (2000) 304.
[4] M. Latroche, R. Baddour-Hadjean, A. Percheron-Guégan, J. Solid State Chem. 173 (2003) 236.

[5] B. Liao, Y.Q. Lei, G.L. Lu, L.X. Chen, H.G. Pan, Q.D. Wang, J. Alloys Compd. 356–357 (2003) 746.
[6] M. Latroche, V. Paul-Boncour, A. Percheron-Guégan, J. Solid State Chem. 177 (2004) 2542.
[7] V.A. Yartys, O. Isnard, A.B. Riabov, L.G. Akselrud, J. Alloys Compd. 356–357 (2003) 109.
[8] V. Paul-Boncour, M. Latroche, A. Percheron-Guégan, J. Solid State Chem. 179 (2006) 3224.
[9] M. Latroche, V. Paul-Boncour, A. Percheron-Guégan, J. Alloys Compd. 404–406 (2005) 60.
[10] R.G. Barnes, in: H. Wipf (Ed.), Hydrogen in Metals, vol. III, Springer, Berlin, 1997, p. 93.
[11] T.T. Phua, B.J. Beaudry, D.T. Peterson, D.R. Torgeson, R.G. Barnes, M. Belhoul, G.A. Styles, E.F.W. Seymour, Phys. Rev. B 28 (1983) 6227.
[12] J. Shinar, D. Davidov, D. Shaltiel, Phys. Rev. B 30 (1984) 6331.
[13] J.T. Markert, E.J. Cotts, R.M. Cotts, Phys. Rev. B 37 (1988) 6446.
[14] A.V. Skripov, Defect Diffus. Forum 224–225 (2003) 75.
[15] A.V. Skripov, A.V. Soloninin, A.L. Buzlukov, L.S. Voyevodina, J.C. Cook, T.J. Udovic, R. Hempelmann, J. Phys. Condens. Matter 17 (2005) 5011.
[16] A.V. Skripov, T.J. Udovic, J.J. Rush, Phys. Rev. B 76 (2007) 104305.
[17] G. Majer, U. Kaess, R.C. Bowman, Phys. Rev. B 57 (1998) 13599.
[18] M.P. Mendenhall, R.C. Bowman, T.M. Ivancic, M.S. Conradi, J. Alloys Compd. 446–447 (2007) 495.
[19] A.C. Switendick, Z. Phys. Chem. N. F. 117 (1979) 89.
[20] R.M. Cotts, in: G. Alefeld, J. Völkl (Eds.), Hydrogen in Metals, vol. I, Springer, Berlin, 1978, p. 227.
[21] L.E. Drain, Proc. Phys. Soc. 80 (1962) 1380.